Neuroinform
DOI 10.1007/s12021-013-9185-2

ORIGINAL ARTICLE

Node Accessibility in Cortical Networks During Motor Tasks

Mario Chavez · Fabrizio De Vico Fallani · Miguel Valencia · Julio Artieda · Donatella Mattia · Vito Latora · Fabio Babiloni

Abstract Recent findings suggest that the preparation and execution of voluntary self-paced movements are accompanied by the coordination of the oscillatory activities of distributed brain regions. Here, we use electroencephalographic source imaging methods to estimate the cortical movement-related oscillatory activity during finger extension movements. Then, we apply network theory to investigate changes (expressed as differences from the baseline) in the connectivity structure of cortical networks related to the preparation and execution of the movement. We compute the topological *accessibility* of different cortical areas, measuring how well an area can be reached by the rest of the network. Analysis of cortical networks reveals specific agglomerates of cortical sources that become less accessible during the preparation and the execution of the finger movements. The observed changes neither could be explained by other measures based on geodesics or on multiple paths, nor by power changes in the cortical oscillations.

Keywords Complex networks · Brain connectivity · Voluntary self-paced movements

Introduction

In neurosciences, it is widely recognized that the brain functioning results from a complex interaction among remote neuronal assemblies (Varela et al. 2001; Bullmore and Sporns 2009).This interaction refers in general to statistical temporal dependences between the activities of different brain regions (Varela et al. 2001) and constitute the basis for the estimation of functional brain connectivity (Horwitz 1994). Although functional connectivity can give a multivariate pattern of interaction between different brain areas that is invisible to standard univariate methods looking at individual activity, (e.g. power spectrum density), it fails in providing an objective and concise description of the topological properties of such a networked system. To this, it has been realized that connectivity patterns can be modeled as graphs, i.e. mathematical objects whose nodes represent different brain regions and links stand for statistically significant bindings between them (Reijneveld et al. 2007; Bullmore and Sporns 2009). This general framework, known as complex network theory, has provided various metrics to characterize the wiring structure at both local (the neighborhood of a node) and global (full network) level (Newman 2003; Boccaletti et al. 2006; da Fontoura Costa et al. 2002). By using graph theoretical approaches, it has been found that functional brain networks obtained from

Electronic supplementary material The online version of this article (doi: 10.1007/s12021-013-9185-2) contains supplementary material, which is available to authorized users.

M. Chavez (✉) · F. De Vico Fallani
CNRS UMR-7225, Hôpital de la Salpêtrière, Paris, France
e-mail: mario.chavez@upmc.fr

D. Mattia · F. Babiloni · F. De Vico Fallani
Department of Human Physiology and Pharmacology,
University "La Sapienza",
Rome, Italy

D. Mattia · F. Babiloni · F. De Vico Fallani
Neuroelectrical Imaging and BCI Lab,
IRCCS "Fondazione Santa Lucia", Rome, Italy

M. Valencia · J. Artieda
Neurophysiology Laboratory, Division of Neurosciences,
CIMA & University of Navarra, Pamplona, Spain

V. Latora
School of Mathematical Sciences, Queen Mary,
University of London, London, UK

functional magnetic resonance imaging (fMRI), magnetoencephalography (MEG) or electroencephalography (EEG) signals display non-random global properties during different mental states. These characteristic attributes identify the so-called "small-world" topology capable to process information within regional clusters avoiding excessive connections between them, and favor an optimal balance between functional segregation and integration (Sporns et al. 2004).

Within this framework, recent metrics have been developed to quantify the influence of a local node over the information spreading within the global brain network (Achard and Bullmore 2007; Valencia et al. 2009; Zamora-López et al. 2009; da Fontoura Costa et al. 2011). Many of these indexes, such as the betweenness centrality and the local efficiency (Newman 2003; Boccaletti et al. 2006) assume that the communication between the nodes of a network takes place only through shortest paths. However, in many real-world networks the information can actually spread over parallel longer pathways (Newman 2005; Estrada and Hatano 2008; Rodrigues and da Fontoura Costa 2010), and different graph indexes have been proposed to take into account the information arising from multiple trajectories in the network (Borgatti 2005; Newman 2005; Noh and Rieger 2004). Interestingly, such information could reflect in neurosciences the concept of redundancy, a natural resource of the brain that would support robust neural interaction and resilience to dysfunctions or damages (De Vico Fallani et al. 2011).

In the light of this consideration, we present a centrality index quantifying the accessibility of a brain region as a function of velocity at which the information flows across the connectivity pattern in terms of random walks. Random walks are the simplest way to explore a graph by considering all the possible alternative pathways, and have been already used to define measures of centrality, for instance by counting the average number of times a given node is visited during a random walk between pairs of vertices (Newman 2005). Here we focus on the hitting time of a node i, defined as the expected time needed by a random walker to reach the node i starting from a generic node j (Lovász 1993). Under the hypothesis that the interactions between different brain regions occur at the same constant velocity, the accessibility of a brain area can be then estimated as the inverse of its hitting time, as this value is inversely proportional to the number and length of the paths performed by the random walker. Differently from methods using an explicit recursive expression of the random walk to obtain the hitting times (Noh and Rieger 2004), here we implement a spectral decomposition that allows a representation in a compact form.

The proposed accessibility index is finally applied to a dataset of high-resolution EEG signals in a group of healthy subjects during the performance of a simple motor act involving the dominant hand. Thanks to advanced source imaging techniques (He et al. 1999; Baillet et al. 2001) we are able to reconstruct large-scale functional networks describing the synchronization between small cortical regions over the entire brain in the standard frequency bands related to the motor acts. In particular, we aim at identifying those cortical areas whose accessibility during the preparation and execution of the motor performance exhibited a significant deviation with respect to a baseline condition. In the remainder of this paper we provide the details of our approach, we summarize the results from an EEG experiment, and we finally discuss their potential implications.

Materials and Methods

Subjects and EEG Recordings

Ten healthy volunteers (mean age 25.7 ± 3.4 years; 3 women) have been recruited for this experiment. All the subjects involved in the experiment were recruited by advertisement. According to the declaration of Helsinki, written informed consent was obtained from each subject after the explanation of the study, which was approved by the local institutional ethics committee of the Scientific Institute for Research, Hospitalization and Health Care, "Fondazione Santa Lucia" in Rome. During the experiment, the participants were comfortably seated in a reclining chair with both arms resting on a pillow in a dimly lit room. They were asked to perform a self-paced brisk extension of the middle finger with their dominant hand (all the subjects were attested as right-handed). Each subject performed 200 movements (trials) in average consecutively; about 6 seconds separated two consecutive movements.

Cerebral activity was recorded with a 61-channel system (BrainAmp, Brain Products GmbH) with a sampling rate of 200 Hz, and referenced to the linked-ear signal. The three-dimensional electrode positions were obtained through a geodesic photogrammetric technique (Cincotti et al. 2008) with respect to anatomic landmarks (nasion and two pre-auricular points). Electrode impedances were set below 15 kΩ. The amplifier bandpass was 0.1 to 70 Hz and the EEG data were later band-pass digitally filtered at 1−45 Hz. Data segments with artifacts due to eye blinks and ocular movements were detected by an expert neurophysiologist and then removed from the original EEG dataset. A semi-automatic procedure was adopted to reject epochs presenting muscular artifacts (Moretti et al. 2003). The motor performance was continuously monitored by recording the EMG signal from the extensor *digitorum communis* (ECD) muscle over the forearm. Off-line, EMG data were digitally high-pass filtered at 20 Hz and rectified. The onset of

each finger movement was then automatically marked based on an amplitude threshold of 30 mV (Brain Vision Analyzer, Brain Products GmbH), and verified through visual inspection by an expert electrophysiologist.

As illustrated in Fig. 1a, for each trial we consider 3 representative temporal epochs of 500 milliseconds of EEG activity: *i)* the baseline period (BASE) starting from 4 seconds before the actual movement onset, *ii)* the preparation epoch (PRE) immediately preceding the EMG onset and, *iii)* the execution period (EXE) following the onset itself. Notably, these periods allow to capture the motor related cortical potentials normally observed in healthy subjects (Ikeda et al. 1992; Pfurtscheller and Lopes da Silva 1999).

Cortical Source Activity from Scalp EEG Signals

Here, we image the cerebral activity underlying the electrodes measurements directly from the single-trial epochs.

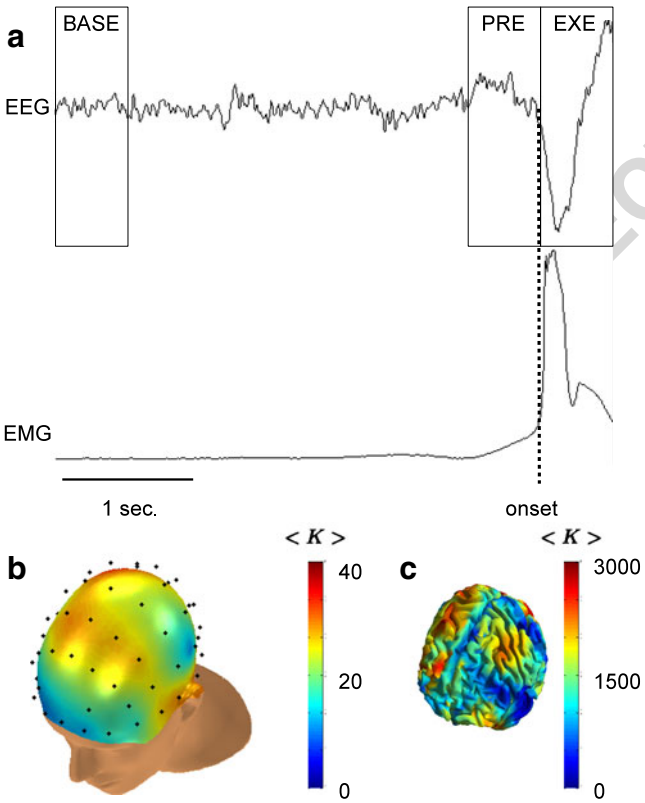

Fig. 1 **a** Averaged EMG and EEG (recorded at the postcentral region) signals of a subject during the execution of finger movements. *Boxes* define the three temporal epochs of EEG activity studied here: baseline (BASE), preparation (PRE) and execution period (EXE). *Vertical dotted line* indicates the movement onset. Examples of scalp and source-level networks obtained from one subject, at the frequency band Beta_1, during the epoch EXE are shown in panels **b** and **c**, respectively. Color map codes the number of connections (i.e. the degree)

To do that, cortical activity was estimated from the segmented 61 EEG signals in each subject through a high-resolution EEG technique, which involves realistic models to characterize the effects of the different electrical conductivities of the head structures and linear inverse solutions (see He et al. 1999 and Baillet et al. 2001 for more details).

White matter/cortical gray matter surface and the interior surface of the skull were segmented from T1-weighted structural MRIs and tessellated with the BrainSuite (http://www.loni.ucla.edu/Software/BrainSuite) package. Statistical comparisons at the population level were done on the basis of the ICBM152 T1 average head model (http://www.loni.ucla.edu/Atlases/). The source model was composed of about 4094 current dipoles, positioned at the vertices of the cortical tessellation, with direction normal to the local pseudo-tangent plane. With this approach, the relevant geometric features are preserved and the orientation of each dipole is constrained to be perpendicular to the cortical mantle, thus modeling the alignment of the pyramidal neurons (Baillet et al. 2001).

The solution of the linear system $\mathbf{Ax} = \mathbf{b} + \boldsymbol{\eta}$ provides an estimate of the dipole source configuration $\mathbf{x}$ that generates the scalp-measured EEG distribution $\mathbf{b}$, with a measurement noise $\boldsymbol{\eta}$, assumed to be normally distributed. The contribution of the whole set of elementary sources is modeled as a spatial transformation matrix $\mathbf{A}$, with as many rows as electrodes and as many columns as cortical sources. Each column j of $\mathbf{A}$ describes the unitary contribution of the dipole j on the potential distribution generated on the scalp electrodes. The coefficients of the matrix A only depend on *i)* the anatomical properties defined by the cortical and head envelopes of the average model, *ii)* the three-dimensional position of electrodes projected over the scalp model for each subject and *iii)* the electrical conductivity of the different tissues of the head.

The source activity can be estimated through the solution ξ of the following linear inverse problem: $\boldsymbol{\xi} = \underset{\mathbf{x}}{\text{argmin}} \left\{ \|\mathbf{Ax} - \mathbf{b}\|^2 + \lambda^2 \|\mathbf{x}\|^2 \right\}$, where the regularization coefficient λ can be considered as both a smoothing parameter and a threshold for the signal-to-noise ratio (Dale and Sereno 1993). Here, we set the value of this parameter to 10 % of the first eigenvalue of $\mathbf{AA}^\top$, where $^\top$ denotes the transposed matrix. The optimal solution of the inverse problem was obtained by constraining the norm of the source space according to the weighted minimum norm algorithm, implemented in the BrainStorm (Baillet et al. 2001) MEG and EEG Toolbox (www.neuroimage.usc.edu/brainstorm). This approach allows thus a fast computation of the magnitude of cortical activities from EEG measurements as matrix $\mathbf{A}$ does not depend on time, and it has to be computed once for each subject. An estimate of the signed magnitude of each dipole composing the cortical model was obtained at

each time sample of the trials of data in each condition (BASE, PRE and EXE). Since the linear inverse procedure mainly depends on the geometrical constraints of the cortex and head, the number of sources has an impact only on the spatial resolution (i.e. a finer or coarser-grained mesh), but little effect on the time courses of the estimated activity. This procedure yielded 500 ms long time windows of cerebral activation at each of the 4094 brain locations (corresponding to the nodes of each subject's individual cortical tessellation). One limitation of this procedure is that all reconstructed networks cover the entire cortical areas of both hemispheres, but exclude subcortical regions and their connections (e.g. the insula or the amygdala).

Source-Level Functional Connectivity

Most of the commonly used measures of functional connectivity such as correlation, spectral coherence and phase locking value, overestimate the magnitude of true connectivity due to the presence of volume conduction and common source effects, a problem that is well known in connectivity studies from scalp EEG time series (Nunez et al. 1997; Srinivasan et al. 1998). Even at the source level, a serious problem in estimating functional connectivity arises from the spurious coherence caused by the leakage of source imaging algorithms (Schoffelen and Gross 2009). To account for spurious connections between a given brain location and its vicinity, functional interactions were obtained from the cortical sources through the computation of the imaginary coherence (iCoh), which overcomes the overestimation biases arising from crosstalk or volume conduction (Nolte et al. 2004). iCoh exploits the fact that spectral components of time series arising from volume conduction, or with a common reference, occur with zero time delay. Thus, by discarding the real component of coherence, one can remove spurious associations and measure the true interactions between brain areas (Nolte et al. 2004).

Given two sources x and y, their imaginary coherence at a certain frequency f can be computed as:

$$\begin{aligned} \mathrm{iCoh}_{xy}(f) &= \mathrm{Im}\left\{\mathrm{Coh}_{xy}\right\} \\ &= \mathrm{Im}\left\{\frac{\sum_{k=1}^{K} X_k(f) Y_k^*(f)}{\sqrt{\sum_{k=1}^{K} \|X_k(f)\|^2 \sum_{k=1}^{K} \|Y_k(f)\|^2}}\right\} \end{aligned}$$

where $X_k(f)$ ($Y_k(f)$) denote the Hanning-windowed, Fourier-transformed segment of trial k at source x (y), with * indicating the complex conjugate. $\|\mathrm{iCoh}_{xy}\|$ provides a bounded and normative evaluation of synchronization, taking values between 0 and 1, with 0 in the case of independence, and 1 in the case of a perfect linear relationship. To normalize the distribution of iCoh values (the variance of Coh_{xy} grows smaller as $\|\mathrm{Coh}_{xy}\|$ gets closer to 1), we used the variance-stabilizing Fisher's Z transform of iCoh_{xy} (Brillinger 2001; Nolte et al. 2004): $Z_{xy} = \mathrm{Im}\left\{\frac{\mathrm{Coh}_{xy}}{\|\mathrm{Coh}_{xy}\|}\right\} 0.5 \ln\left(\frac{1+\|\mathrm{Coh}_{xy}\|}{1-\|\mathrm{Coh}_{xy}\|}\right)$. This procedure yields a transformed coherence with an approximately constant variance given by $\frac{1-\|\mathrm{Coh}_{xy}\|^2}{2K} \frac{\mathrm{arctanh}^2\left(\|\mathrm{Coh}_{xy}\|^2\right)}{\|\mathrm{Coh}_{xy}\|^2}$, where K is the number of trials.

Here we study the level of synchronization between cortical signals in the following standard physiological frequency bands: Alpha (7.5–12.5 Hz), Beta_1 (12.5–20.5 Hz), Beta_2 (20.5–29.5 Hz) and Gamma (29.5–40.5 Hz). The choice of these frequency bands was on the basis of previous findings indicating that changes of these activities are mainly involved in finger movements (Leocani et al. 1997; Pollok et al. 2006).

Construction of Connectivity Graphs

Synchronization values for frequency bands are calculated from the average of Z_{xy} values of the corresponding frequency bins, generating thus a single value for each frequency band of interest. For each epoch, frequency band and subject, we obtain a connectivity matrix $\mathbf{W}$ with entries $w_{ij} = \|Z_{ij}\|$ accounting for the whole brain (cortical surface) network. Each element w_{ij} codes thus the intensity of the synchronization between the signals from two cortical sources i and j.

At this stage, the functional brain connectivity is a fully connected and undirected network. Each matrix of 4094 × 4094 synchronization values is converted into a weighted adjacency matrix $\mathbf{\Gamma}$ by applying a threshold Γ_{th} such that the number of links in the matrix was fixed according to a constant density of links (often called cost). The weight of the link between i and j is set such that $\Gamma_{ij} = w_{ij}$ if $w_{ij} > \Gamma_{th}$, and $\Gamma_{ij} = 0$ otherwise (diagonal elements were set to $\Gamma_{ii} = 0$). This approach allows comparing network properties at different frequency bands and epochs, while controlling for effects of connection density on network topology (van Wijk et al. 2010).

Here, as every node must be accessible at least by one link, the link density is defined on the basis of the minimal threshold Γ_{th} above which all the graphs were connected, i.e. there is a path from any point to any other point in the graph. The density of links is thus fixed at 35 % for all the networks considered in this study. We notice that some recent works have pointed out the effects of such approach (fixing an arbitrary edge density or a range of densities) on the measured network properties, mainly due to the statistical significance of the estimator of functional connectivity (Toppi et al. 1989; Langer et al. 2013). To

determine to which extent non-significant connectivity values are included in our networks, we have applied a statistical significance test to coherence values, followed by a False Discovery Rate (FDR) method to correct for multiple testing (Brillinger 2001; Nolte et al. 2004). With this approach, the threshold of significance is set such that the expected fraction of false positives is restricted to $q \leq 0.05$. For a FDR threshold based on tests independence (Benjamini and Hochberg 1995), the average density of links across subjects, conditions and frequency bands was 43 %, while a much more conservative FDR procedure that assumes weak dependencies between tests (Benjamini and Yekutieli 2001) yielded an average density of 22 %. The threshold used to ensure a connected graph is therefore more conservative than a simple correction for multiple tests, but more permissive than the refined FDR procedure. An example of the obtained brain networks during the execution of voluntary movements is depicted in Fig. 1b–c.

Node Accessibility

Random walks constitute a simple way to model a signal originating at a single node and spreading through a graph. When random walker moves on a network, at each time step, the probability of jumping from an occupied node i to a node j, can be represented by $P_{ij} = \Gamma_{ij}/s_i$, where $s_i = \sum_k \Gamma_{ik}$ is the strength of node i. In matrix form, we can write the matrix $\mathbf{P} = \{P_{ij}\}$ as $\mathbf{P} = \mathbf{D}\boldsymbol{\Gamma}$, where $\mathbf{D}$ is the diagonal matrix of inverse nodes strengths $D_{ii} = s_i^{-1}$. As a result, the random sequence of nodes $\{v_t : t = 0, 1, \ldots\}$ occupied by the walkers at consecutive times is a Markov chain with $\mathbf{P}$ as transition matrix.

If we denote by $\boldsymbol{\mu}(t)$ the distribution of v_t in the Markov chain, i.e. $\mu_i(t) = \Pr(v_t = i)$, the rule of the walk can be expressed by $\boldsymbol{\mu}(t+1) = \mathbf{P}^\top \boldsymbol{\mu}(t)$. For an undirected and connected graph, the Perron Frobenius theorem assures that $\mu_i^* = \dfrac{s_i}{\sum_k s_k}, i = 1, \ldots, N$, is the unique stationary distribution of the Markov chain, such that $\lim_{t\to\infty} \sum_i p_{ij}(t)\mu_i(0) = \mu_j^*, i = 1, \ldots, N$, for any initial distribution $\boldsymbol{\mu}(0)$ (Chung 1997).

Here, we characterize the velocity at which information flows across a network in terms of random walks, as defined above. The *access time* H_{ij}, also known as hitting time, is the expected number of steps before node j is visited, starting from node i. Using the spectral decomposition of matrix Π, the elements H_{ij} can be computed for each pair of nodes i, j as (Lovász 1993):

$$H_{ij} = 2S \sum_{k=2}^{N} \frac{1}{1-\lambda_k} \left(\frac{\varphi_{ki}^2}{s_i} - \frac{\varphi_{ki}\varphi_{kj}}{\sqrt{s_i s_j}} \right)$$

where $\lambda_1 = 1 \geqslant \lambda_2 \geqslant \cdots \geqslant \lambda_N$ are the eigenvalues of the symmetric matrix $\boldsymbol{\Pi} = \mathbf{D}^{-1/2}\boldsymbol{\Gamma}\mathbf{D}^{1/2}$ and $\varphi_1, \ldots, \varphi_N$ are the corresponding eigenvectors, and $S = \sum_i s_i$ is the total strength of the network, i.e. the sum of the strengths of all nodes s_i.

We can define the average access time h_j of a given node j as the average time it takes to reach node j from the rest of the network: $h_j = N^{-1} \sum_i^N H_{ij}$. For homogeneous and symmetric networks, e.g. random graphs, all nodes have the same accessibility, whereas the distribution of the accessibility in heterogeneous connectivities is ruled by the induced asymmetry of the dynamic process (random walk). Assuming that the facility in the communication between i and j is inversely proportional to the access times H_{ij}, we can define the *accessibility of node* j as $a_j = \dfrac{1}{h_j}$. Since access times take values that can vary in the range $[1, \infty)$, the quantity a lies in the interval $[0, 1]$.

Notice that, in contrast with metrics based on shortest paths, the access time H_{ij} reflects how the information flow passes through all possible routes. Indeed, the hitting time from node i to node j has the property of decreasing when the number of paths from i to j increases and the lengths of the paths decrease (Doyle and Snell 1984).

A related concept of communicability has been defined by Estrada and Hatano (2008), Estrada et al. (2009) to measure the ability of information to flow across the network. Such communicability measure is based on the exponential of the adjacency matrix and it also assumes that the spreads of information is not restricted to only shortest paths. Nevertheless this metrics has been shown to be sensitive to undue effects of heterogeneity of degree/strengths of nodes (Crofts and Higham 2009). Similarly, the centrality measure proposed by Noh and Rieger (2004), also based on random walks, reflects the global structure of the network as the accessibility. Nevertheless, its estimation uses an explicit recursive expression of the random walk for obtaining the hitting times, whereas the spectral decomposition used here allows us to represent it in a compact form.

Importance of Multiple Shortest Paths

To illustrate the concept of accessibility, we consider the two graphs represented in Fig. 2. The first one illustrates the case in which a node, like c, may play a key role in the flow of information between the different nodes of the network, despite its weak number of connections. The second example shows a prototype of networks in which there are some nodes, like c, which are not intermediaries in many shortest paths, but play a central role in the flow of information between different groups. Betweenness centrality, which is an index based on the shortest path length (see definition below) is compared with accessibility values in Fig. 2. We

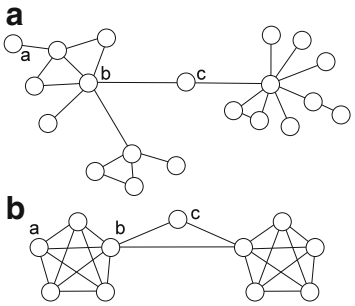

Network	Node	Degree	BC	a
A	a	1	0	0.012
	b	6	0.66	0.044
	c	2	0.52	0.040
B	a	4	0	0.047
	b	6	0.533	0.093
	c	2	0	0.043

Fig. 2 Graphs used to explain the differences between different centrality measures: accessibility, betweenness centrality metrics (as a measure based on the trivial shortest paths lengths) and degree (as a measure based local neighborhood). The table on the right indicates such values for different nodes. **BC** and **a** stand for betweenness centrality and accessibility, respectively

see that for network A, both measures indicate that node c, despite its few number of connections, plays the most significant role for the communication of the network. For network B, shortest path analysis indicates that nodes a and b play no role in the communication. Nevertheless, although node c is never an intermediary in a shortest length walk, it may play a non-trivial role in the spread of information in the whole network. We see that accessibility is able to describe the role played by this node in the network communication, by taking into account interactions related to longer non-trivial pathways.

Statistical Contrast Between Motor and Baseline Conditions

To perform statistical testing at the population level, the cerebral data need to be warped to a common anatomical space, such as the standard Montreal Neurological Institute (MNI) brain. Here, scalp locations of anatomical landmarks (nasion, vertex and two preauricular points) on each participant were identified on the MNI averaged brain (http://www.mni.mcgill.ca), and the brain location of EEG sources were estimated by projection into anatomical coordinates of the MNI brain. Although this approach leads to a limited accuracy with regard to the anatomical precision of the source locations, the mean difference in Talairach coordinates between estimates using the real scalp and the averaged MNI scalp locations has been found to be less than 1 cm, and typically 4−6 mm (Pollok et al. 2002), which provides an acceptable approximation for the purposes of our study. In this work, the standardized averaged MNI brain was used trough the whole analysis (sources estimation, multiple comparisons and group statistics) but, for visualization purposes, in Figs. 3 and 4 we projected the statistical maps into the MRI of one subject.

To assess significant differences between topological features of different conditions we contrast cortical maps of two pairs of epochs (BASE vs PRE and BASE vs EXE) over subjects. For this, we use standard nonparametric permutation methods, which randomly exchanged the estimated topological indices in any pair of epochs for each subject (Bullmore et al. 1999; Pantazis et al. 2005). We use exhaustive permutations $\left(2^{10}\right)$ to estimate the empirical distribution under the null hypothesis of no difference between any two periods. The standard statistical procedures that operate at the level of single sources have the disadvantage of neglecting the spatially coordinated nature of imaging data. Further, due to the large number of statistical comparisons (the number of sources), it is not possible to control the so-called family-wise error rate (FWER). To circumvent this problem, we use here cluster-based statistics, which are more informative than source-level statistics about the neuroanatomical differences between small groups of subjects (Bullmore et al. 1999; Hayasaka and Nichols 2003). Difference maps at the source-level are thresholded first at $p \leq 0.05$ by using group-level ($n = 10$), one-tailed paired permutation tests, to give maximum sensitivity and to avoid type II errors. Next, the significance threshold of clusters-mass (defined by the sum of all suprathreshold values within the cluster) is adjusted to the maximum statistic distribution of cluster masses in the paired-permuted data. This procedure corrects the FWER such that the final expected number of type I error clusters under the null hypothesis is less than 1 over the entire brain surface. Cluster mass rather than a cluster extent threshold is used here, to minimize discrimination against possible small but significantly different brain regions (Bullmore et al. 1999).

Comparison with Other Source-Level Local Measures and with Random Graphs

Together with the standard power spectrum estimates of cortical activity (P), different centrality measures account for different aspects of the topological relevance of a node.

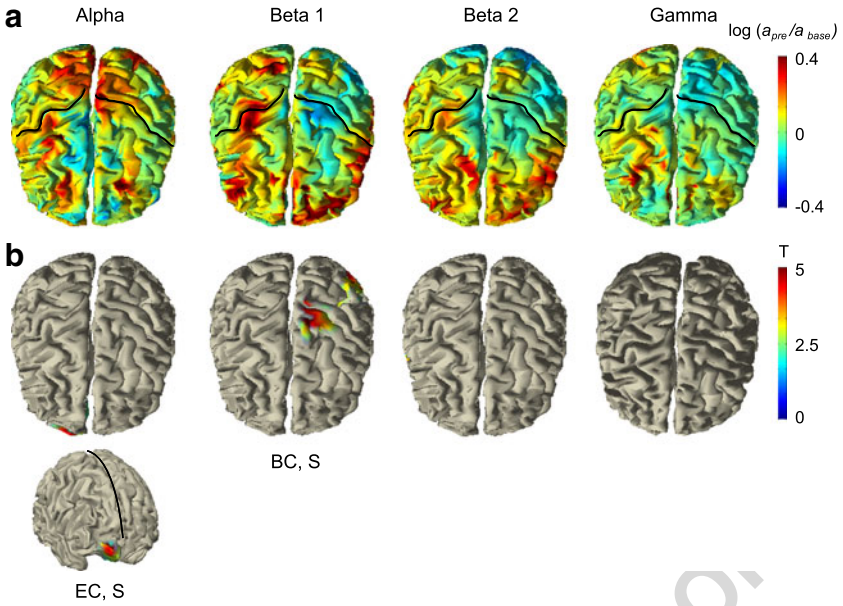

Fig. 3 Changes in cortical accessibility between the temporal epochs BASE and PRE. **a** Averaged changes in accessibility estimated as the ratio (in log scale) of a values in the epochs BASE and PRE, for the frequency bands Alpha, Beta_1 , Beta_2 and Gamma. *Black lines* on these cortical maps indicate the central sulcus. **b** Corresponding T-values maps of statistical differences: clusters with significant differences ($p < 0.05$, corrected) are overlaid on a template brain. Picture at the bottom correspond to rotated representation of the cortex for better illustration of the small significant area (the medial longitudinal fissure is indicated by a *black line*). The text labels below the cortical maps indicate other topological measures that also display significant differences in the same cortical regions: betweenness centrality (BC), eigenvector centrality (EC), information centrality (IC), pagerank (PR), power of cortical oscillations (P), or strength (S)

Here, we also study the changes of connectivity at the node level by also computing standard metrics, such as the average distance from a node to the other graph nodes (SPL), the clustering index of each node (CC), and its strength (S). We also use other standard centrality measures based on shortest paths and on paths of any length, and some spectral centrality measures. Following is the list.

- The betweenness centrality (BC) of a node i is defined as $BC(i) = \sum_{\substack{j,k \\ j\neq k\neq i}} \frac{n_{jk}(i)}{n_{jk}}$, where n_{jk} is the number of shortest paths connecting nodes j and k, while $n_{jk}(i)$ is the number of shortest paths connecting j and k and passing through i (Freeman 1977). Thus, it basically reflects the extent to which communication between nodes in a network depend on a given node.
- The information centrality (IC) of a node i is defined as the harmonic average of its distance to the other nodes in the graph: $IC(i) = \left(\frac{1}{N}\sum_j \frac{1}{I_{ij}}\right)^{-1}$, where $I_{ij}^{-1} = (BB^{-1})_{ii} + (BB^{-1})_{jj} - 2(BB^{-1})_{ij}$ (Stephenson and Zelen 1989). Entries $(B^{-1})_{ij}$ can be obtained by inverting the matrix $\mathbf{B} = \mathbf{D}^{-1} - \mathbf{\Gamma}$. While BC focuses just on geodesic, IC takes into account how information might flow through all paths linking a pair of nodes, weighted by the the length of the paths.
- The eigenvector centrality (EC) is defined as the principal eigenvector of the adjacency matrix $\mathbf{\Gamma}$ of the graph (Bonacich 1972). Eigenvector centrality can be seen as a generalization of the degree, that iteratively defines and quantifies the importance of a node as being proportional to the importance of its first neighbors. Thus, it takes into account the entire connectivity of the graph.
- Finally, PageRank centrality (PR) is a well known measure of importance or prestige of Web pages. PR is a variant of the EC and its values are the entries of the dominant eigenvector of the modified matrix $\mathbf{G} = \delta\mathbf{P} + \frac{(1-\delta)}{N}\mathbf{e}\mathbf{e}^\top$, where $\mathbf{e}^\top$ is a vector of all 1s, and the scalar δ controls the probability to randomly jump to any node in the network (here, we set $\delta = 0.85$).

To assess the significance of nodes' accessibility observed in cortical networks, we generate a benchmark comparison of the functional connectivity patterns. To do this, accessibility values of brain networks are compared with those obtained from equivalent random configurations. To create such an ensemble of surrogate networks, each weighted edge of the original network is randomly shuffled avoiding self- and duplicate connections. Although there are more refined algorithms satisfying a specific set of constraints (namely the degree sequence), they cannot be easily extended to cover the strength sequence. Further, existing

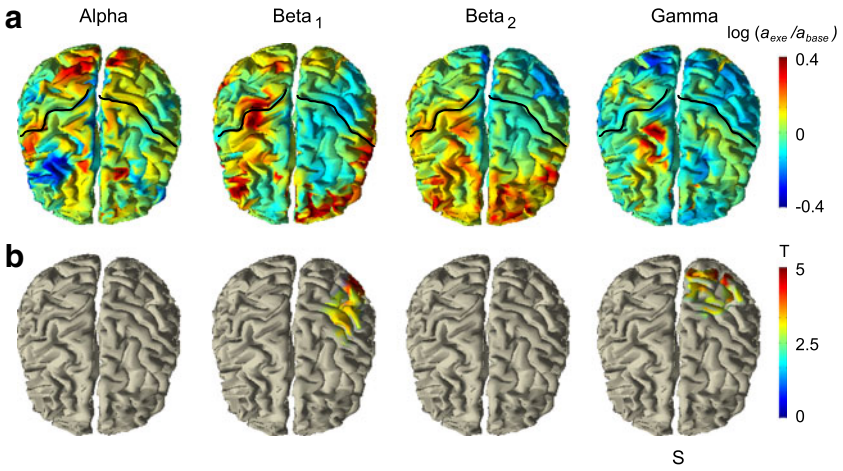

Fig. 4 Changes in cortical accessibility between the epochs BASE and EXE. **a** Averaged changes in accessibility estimated as the ratio (in log scale) of a values in the epochs BASE and PRE, for the frequency bands Alpha, Beta_1 , Beta_2 and Gamma. *Black lines* on these cortical maps indicate the central sulcus. **b** Corresponding T-values maps of statistical differences: clusters with significant differences ($p < 0.05$, corrected) are overlaid on a template brain. The text label below the cortical maps corresponds to the strength (S), the topological measure that also displays significant differences in the same cortical regions

algorithms are extremely demanding in terms of computation time (Ansmann and Lehnertz 2011). The randomized networks used in our study have the same distribution of weights (and the same number of links) as the original network.

Results

Results obtained in the preparation (PRE) period are illustrated in Fig. 3, whereas Fig. 4 shows the results obtained for the execution (EXE) period. The most interesting results are observed in the Beta_1 band ($12 - 20$ Hz), where a significant decrease ($p < 0.05$, corrected) of accessibility is reported for the cortical sources of the contralateral hemisphere in both the preparation (PRE) and execution (EXE) period with respect to the baseline (BASE). In particular, in the PRE condition the loss of accessibility is mainly located in parts of the primary motor cortex of the hand (Broadmann's area 4 or BA4) and in portions of the parietal regions BA39 and BA40; these parietal regions also exhibit a similar significant difference in the EXE condition, where a moderate shift from the primary motor area to the sensory cortex of the hand (BA1-2-3) is observed in terms of significant decrease of accessibility.

In the Gamma band ($30 - 40$ Hz), only the reconfiguration of cortical networks in the EXE period yields a significant ($p < 0.05$, corrected) decrease of accessibility in parts of the contralateral sensorimotor cortex of the hand (BA1-2-3-4), and parietal BA5 and and BA7. In the Alpha band ($7 - 12$ Hz) we observe a significant loss of accessibility only in the PRE condition for the cortical sources belonging to the ipsilateral frontopolar areas, namely BA10 and BA11. No other statistically significant changes are observed in the other frequency ranges.

Notably, all the estimated functional brain networks exhibit a critical deviation from typical random graphs in terms of accessibility. Differently from what we observe in the real cortical networks the distribution of a values of surrogate networks is found to display a high spatial homogeneity for all the epochs considered (BASE, PRE and EXE) and for all frequency bands (10 surrogate networks were generated for each condition). The distribution of a values from all surrogate networks of all subjects is centered at $|\log a| \sim 3.6$ with a very small standard deviation ($\sim 10^{-7}$ estimated over all cortical sources) hundred of times smaller than real cortical networks. Although the preparation and execution of movements may be accompanied by changes in the global amount of cortical synchrony, if real networks are randomly rewired by keeping the same distribution of weights, no differences in accessibility are observed between any condition.

Regions with significant differences in accessibility ($p < 0.05$, corrected) are depicted in Figs. 3b and 4b. Topological indices detecting differences in the same regions are indicated by the corresponding labels just below the cortical maps of accessibility differences. Although the spatial extent of such changes are qualitatively the same as those observed in the accessibility values (the spatial overlap between the corresponding BAs is of at least 85 %), results show that other centrality measures (BC, EC, IC or PR) do not reveal the whole set of areas detected by accessibility. Moreover, neither geodesics and clustering index, nor the local power of cortical activities, reveal any

significant change either (at any frequency or condition). Although *most* of the connectivity changes observed in the accessibility values can be also detected by the local strength, accessibility is able to detect nodes with non-trivial interactions related to multiple pathways, such as those illustrated in Fig. 2. To assess whether such connectivity modifications are related to the local neighborhood of each node, we also evaluate the clustering index, which is related to the local ÓcliquenessÓ of nodes. Result show no changes on this index suggesting that connectivity changes were not in the local neighborhood of nodes.

Discussion

Despite the large literature about changes of oscillatory activities during voluntary motor tasks (Pfurtscheller and Lopes da Silva 1999; Cassidy et al. 2002), only in recent years we have witnessed a growing interest in the study of their functional organization in brain networks (Eguíluz et al. 2005; Bassett et al. 2006; De Vico Fallani et al. 2008; Jin et al. 2012). Using a graph theoretical approach, we characterize the large-scale functional brain networks obtained during the preparation and execution of self-paced finger extensions in a group of healthy subjects by means of a centrality index quantifying how well each cortical area is "accessible" by the rest of the network.

As expected, accessibility of cortical networks is different from random configurations (with the same link weight distributions), in which all the nodes exhibit a largely homogeneous accessibility over all the cortical sources. This rules out the possibility that differences in the strength of synchronization alone could account for differences in the accessibility of cortical areas. Our results show that, although centrality measures (BC, EC, IC and PR) are relatively correlated between them, and with the accessibility values (see Online Resources), they generally do not reveal significant changes between the conditions. This can be explained by the fact that they have larger variability across subjects than accessibility. The theoretical explanation of correlations between network metrics, as well as variability of topological estimators are not studied here, but they remain a challenging topic for future studies.

Results suggest that the strength of nodes may provide complementary information about modification in the connectivity of brain networks. Indeed, this is in agreement with the dependence found in (Noh and Rieger 2004) between the hitting times and the node degree. Nevertheless, we must notice that the strength of a node accounts for a very local aspect of the topological relevance of a node, whereas accessibility accounts for global structure explored by all possible routes between nodes. Differently from other centrality measures based on shortest path lengths, accessibility rather relies on all possible walks of any length, and it therefore accounts for the non-trivial interactions via longer paths.

Whereas the use of graph tools seem to be particularly adequate to characterize brain networks, the estimation of connectivity patterns from EEG data may be limited due to the fact that the electromagnetic field generated by a given neural source is simultaneously measured at multiple EEG electrodes. Nearby EEG recording sites are thus likely to pick up activity of common sources, resulting in strong interactions between recorded signals that reflect simple volume conduction rather than true functional connectivity (Nunez et al. 1997; Srinivasan et al. 1998). To overcome this limitation, we estimate here the cerebral sources of EEG activity using an inverse problem solution, spatially constraining the locations of the sources on the cortical mantle (He 1998; Baillet et al. 2001).

Although brain imaging methods are a useful tool for studying functional interactions in the brain, they may present some limitations. Interactions are currently based on few regions-of-interest that are selected based on specific criteria such as synchronization to an external reference channel (Gross et al. 2002), or by contrasting levels of sources' activities (e.g. power of oscillations) between experimental conditions (Gross et al. 2004). Here we determine a large cortical network directly from interactions among all cortical sources, without prior assumptions of specific areas.

The use of the imaginary coherence for computing the functional connectivity between all the cortical source activities has some advantages in this study. First, being a bivariate measure it does not require particularly long time windows (i.e. trials in this study) to estimate in a reliable way connectivity patterns with large number of nodes. Although other multivariate measures are more robust to the identification of spurious links (e.g. Directed Transfer Function or Partial Directed Coherence) between a reduced number of nodes (Imamoglu et al. 2012), they need relatively longer data for the estimation of large scale networks as those considered in our study (Astolfi et al. 2005; Schlögel and Supp 2006). Second, as a measure capable to isolate volume conduction bias, it is appropriate to compute functional connectivity between sources which are geometrically close and that could be affected by possible residual field spread and cross-talk effects after the linear inverse procedure (Schoffelen and Gross 2009).

Here, we find that a significant ($p < 0.05$, corrected) decrease of accessibility occur in the Beta_1 band for the cortical regions of the contralateral hemisphere in both the PRE and EXE period. These regions include parts of the primary sensorimotor areas (BA 1-2-3-4) of the hand which are largely known to be central for the performance of motor acts (Pfurtscheller and Lopes da Silva 1999; Ohara et al. 2001; Mattia et al. 2009) and secondary sensory parietal

areas (BA 39–40), which appear to be involved in higher order cognitive motor functions, including understanding of intention (Wolpert et al. 1995; Fogassi and Luppino 2005). Our results agree with other scalp EEG studies reporting the involvement of the primary sensorimotor cortex during finger-tapping tasks (Bai et al. 2005; Jin et al. 2012). Interestingly, the observed decrease of accessibility in the Beta_1 band reflect a higher tendency of specific portions of the motor-related cortical areas to get isolated from the rest of the network. Such a behavior could be associated to a necessary and temporary stronger interaction with the subcortical structures, as the basal ganglia and the cerebellum, which typically implement complementary mechanisms integrating the motor-related activity during the movement performance (Middleton and Strick 2000).

In the Gamma band only the EXE condition exhibits a significant ($p < 0.05$, corrected) loss of accessibility in cortical patches belonging to the contralateral primary sensorimotor areas (BA 1-2-3-4) of the hand and to the somatosensory associative areas (BA 5, 7). This accessibility decrease indicates a higher tendency of the cortical areas to get isolated (segregated) from the rest of the network. Previous studies Cheyne et al. (2008) proposed that cortical Gamma oscillations observed in primary motor cortex during self-paced movements reflect the activation of local cortico-subcortical interactions involved in the feedback control of discrete movements. On the basis of these studies, our results could suggest that the local recruitment of these cortical areas play a role in sensorimotor integration during the execution of movements. Furthermore, these findings support the hypothesis that Gamma oscillations play a role in a relatively late stage of motor control, by encoding information related to limb movement rather than to muscle contraction (Muthukumaraswamy 2010).

In the Alpha band we only find significant ($p < 0.05$, corrected) decrease of accessibility during the PRE period in small portions of the prefrontal BA 10 and BA 11 ipsilateral to the movement. From a general perspective, the role of prefrontal cortices during simple self-paced movements have been suggested to be similar to those already involved in working memory tasks (Baker et al. 2011). In particular, the authors of that study proposed that the pre-movement period preceding voluntary actions could reflect the engage of control cortical mechanisms for the initiation of such voluntary act. Thus, we speculate that the observed changes in the accessibility of such prefrontal cortical areas could be related to the possible cognitive control mechanisms implicated in a very simple self-paced movement, like the finger extension here studied.

From our results we finally conclude that the application of graph theoretical analysis to sensorimotor task-related functional networks would be helpful in extending our understanding of sensorimotor processing in terms of functional integration. Our findings suggest that the characterization of brain networks can be improved by exploiting the information contained in the flow that passes through all possible paths between the nodes. Interestingly, none of the connectivity indices were correlated with the local power of cortical oscillations, for all conditions and frequency bands. This supports the hypothesis that motor control is not only related to a functional localization but to a coordination of functional segregated brain regions at different frequency bands.

Information Sharing Statement

Data and software code are publicly available in our website at https://sites.google.com/site/fr2eborn/download

- The MATLAB routine for estimating the hitting times H_{ij}. Redistribution and modification of this routine is permitted under the terms of the GNU General Public License
- Different matrices with the values of $w_{ij} = \|Z_{ij}\|$, averaged over all the subjects, for the three conditions (BASE, PRE, EXE), and the frequency bands (Alpha, Beta1, Beta2 and Gamma). Data are in MATLAB format.

Acknowledgments This study was supported in part by Cochlear Inc. and by a grant of "Ministero dell'Istruzione, dell'Universita e della Ricerca", Direzione Generale per l' Internazionalizzazione della Ricerca, in a bilateral project between Italy and Hungary. M. V. acknowledges financial support from the Spanish Ministry of Science and Innovation; Juan de la Cierva Programme Ref. JCI-2010-07876. F. D. V. F. is founded by the French program "Investissements d'avenir" ANR-10-IAIHU-06. M.V. and M.C. acknowledge financial support from the Gobierno de Navarra, Education Department, Jerónimo de Ayanz Programme M. C. thanks to the CIMA and University of Navarra, for their kind hospitality during the different visits for the preparation of this work.

Conflict of Interest The authors declare that they have no conflict of interest.

References

Achard, S., & Bullmore, E. (2007). Efficiency and cost of economical brain functional networks. *PLoS Computational Biology*, *3*, e17.

Ansmann, G., & Lehnertz, K. (2011). Constrained randomization of weighted networks. *Physical Review E*, *84*, 026103.

Astolfi, L., Cincotti, F., Mattia, D., de Vico Fallani, F., Lai, M., Baccala, L., Salinari, S., Ursino, M., Zavaglia, M., Babiloni, F. (2005). Comparison of different multivariate methods for the estimation of cortical connectivity: Simulations and applications to EEG data. In *Conference proceedings of the IEEE engineering in medicine and biology society* (pp. 4484–4487).

Bai, O., Mari, Z., Vorbach, S., Hallet, M. (2005). Asymmetric spatiotemporal patterns of event-related desynchronization preceding

voluntary sequential finger movements: a high-resolution EEG study. *Clinical Neurophysiology*, *116*, 1213–1221.

Baillet, S., Mosher, J., Leahy, R. (2001). Electromagnetic brain mapping. *IEEE Signal Processing Magazine*, *18*, 14–30.

Baker, K.S., Mattingley, J.B., Chambers, C.D., Cunnington, R. (2011). Attention and the readiness for action. *Neuropsychologia*, *49*(12), 3303–3313.

Bassett, D.S., Meyer-Lindenberg, A., Achard, S., Duke, T., Bullmore, E. (2006). Adaptive reconfiguration of fractal small-world human brain functional networks. *Proceedings of the National Academy of Sciences of the United States of America*, *103*, 19518–19523.

Benjamini, Y., & Hochberg, Y. (1995). Controlling the false discovery rate: a practical and powerful approach to multiple testing. *Journal of the Royal Statistical Society: Series B*, *57*, 289–300.

Benjamini, Y., & Yekutieli, D. (2001). The control of the false discovery rate in multiple testing under dependency. *Annals of Statistics*, *29*, 1165–1188.

Boccaletti, S., Latora, V., Moreno, Y., Chavez, M., Hwang, D.-U. (2006). Complex networks: structure and dynamics. *Physics Reports*, *424*, 175–308.

Bonacich, P. (1972). Factoring and weighting approaches to status scores and clique identification. *Journal of Mathematical Sociology*, *2*, 113–120.

Borgatti, S.P. (2005). Centrality and network flow. *Social Networks*, *27*, 55–71.

Brillinger, D.R. (2001). *Time series: Data analysis and theory*. Philadelphia: SIAM.

Bullmore, E., & Sporns, O. (2009). Complex brain networks: graph theoretical analysis of structural and functional systems. *Nature Reviews Neuroscience*, *10*, 1–13.

Bullmore, E.T., Suckling, J., Overmeyer, S., Rabe-Hesketh, S., Taylor, E., Bramme, M.J. (1999). Global, voxel, and cluster tests, by theory and permutation, for a difference between two groups of structural MR images of the brain. *IEEE Transactions on Medical Imaging*, *18*, 32–42.

Cassidy, M., Mazzone, P., Oliviero, A., Insola, A., Tonali, P., Di Lazzaro, V., Brown, P. (2002). Movement-related changes in synchronization in the human basal ganglia. *Brain*, *125*, 1235–1246.

Cheyne, D., Bells, S., Ferrari, P., Gaetz, W., Bostan, A.C. (2008). Self-paced movements induce high-frequency gamma oscillations in primary motor cortex. *Neuroimage*, *42*(1), 332–342.

Chung, F.R.K. (1997). *Spectral graph theory*. Providence: American Mathematical Society.

Cincotti, F., Mattia, D., Aloise, F., Bufalari, S., Astolfi, L., De Vico Fallani, F., Tocci, A., Bianchi, L., Marciani, M.G., Gao, S., Millan, J., Babiloni, F. (2008). High-resolution EEG techniques for brain-computer interface applications. *Journal of Neuroscience Methods*, *167*, 31–42.

Crofts, J.J., & Higham, D.J. (2009). A weighted communicability measure applied to complex networks. *Journal of the Royal Society Interface*, *6*, 411–414.

da Fontoura Costa, L., Rodrigues, F.A., Travieso, G., Boas, P.R.V. (2002). Characterization of complex networks: a survey of measurements. *Advances in Physics*, *56*, 167–242.

da Fontoura Costa, L., Batista, J.L.B., Ascoli, G.A. (2011). Communication structure of cortical networks. *Frontiers in Computational Neuroscience*, *5*, 6.

Dale, A.M., & Sereno, M.I. (1993). Improved localisation of cortical activity by combining EEG and MEG with MRI cortical surface reconstruction: a linear approach. *Journal of Cognitive Neuroscience*, *5*, 162–176.

De Vico Fallani, F., Astolfi, L., Cincotti, F., Mattia, D., Marciani, M.G., Tocci, A., Salinari, S., Witte, H., Hesse, W., Gao, S., Colosimo, A., Babiloni, F. (2008). Cortical network dynamics during foot movements. *Neuroinformatics*, *6*(1), 23–34.

De Vico Fallani, F., Rodrigues, F.A., da Fontoura Costa, L., Astolfi, L., Cincotti, F., Mattia, D., Salinari, S., Babiloni, F. (2011). Multiple pathways analysis of brain functional networks from EEG signals: an application to real data. *Brain Topography*, *23*, 344–354.

Doyle, P.G., & Snell, L. (1984). *Random walks and electric networks,*. Washington: The Mathematical Association of America.

Eguíluz, V.M., Chialvo, D.R., Cecchi, G.A., Baliki, M., Apkarian, A.V. (2005). Scale-free brain functional networks. *Physical Review Letters*, *94*, 018102.

Estrada, E., & Hatano, N. (2008). Communicability in complex networks. *Physical Review E*, *77*, 036111.

Estrada, E., Higham, D.J., Hatano, N. (2009). Communicability betweenness in complex networks. *Physica A*, *388*, 764–774.

Fogassi, L., & Luppino, G. (2005). Motor functions of the parietal lobe. *Current Opinion in Neurobiology*, *15*, 626–631.

Freeman, L.C. (1977). A set of measures of centrality based on betweenness. *Sociometry*, *40*, 35–41.

Gross, J., Timmermann, L., Kujala, J., Dirks, M., Schmitz, F., Salmelin, R., Schnitzler, A. (2002). The neural basis of intermittent motor control in humans. *Proceedings of the National Academy of Sciences of the United States of America*, *99*, 2299–2302.

Gross, J., Schmitz, F., Schnitzler, I., Kessler, K., Shapiro, K., Hommel, B., Schnitzler, A. (2004). Modulation of long-range neural synchrony reflects temporal limitations of visual attention in humans. *Proceedings of the National Academy of Sciences of the United States of America*, *101*, 13050–13055.

Hayasaka, S., & Nichols, T.E. (2003). Validating cluster size inference: random field and permutation methods. *Neuroimage*, *20*, 2343–2356.

He, B. (1998). High-resolution source imaging of brain electrical activity. *IEEE Engineering in Medicine and Biology Magazine*, *17*, 123–129.

He, B., Wang, Y., Wu, D. (1999). Estimating cortical potentials from scalp EEG's in a realistically shaped inhomogeneous head model by means of the boundary element method. *IEEE Transactions on Biomedical Engineering*, *46*, 1264–1268.

Horwitz, B. (1994). The elusive concept of brain connectivity. *Neuroimage*, *19*, 466–470.

Ikeda, A., Lüders, H.O., Burgess, R.C., Shibasaki, H. (1992). Movement-related potentials recorded from supplementary motor area and primary motor area. Role of supplementary motor area in voluntary movements. *Brain*, *115*, 1017–1043.

Imamoglu, F., Kahnt, T., Koch, C., Haynes, J.-D. (2012). Changes in functional connectivity support conscious object recognition. *Neuroimage*, *63*, 1909–1917.

Jin, S.H., Lin, P., Hallett, M. (2012). Reorganization of brain functional small-world networks during finger movements. *Human Brain Mapping*, *115*, 861–872.

Langer, N., Peroni, A., Jäncke, L. (2013). The problem of thresholding in small-world network analysis. *PLoS ONE*, *8*, e53199.

Leocani, L., Toro, C., Manganotti, P., Zhuang, P., Hallett, M. (1997). Event-related coherence and event-related desynchronization/synchronization in the 10 hz and 20 Hz EEG during self-paced movements. *Clinical Neurophysiology*, *104*, 199–206.

Lovász, L. (1993). Random walks on graphs: A survey. In D. Miklos, V.T. Sos, T. Szonyi (Eds.), *Combinatorics, Paul Erdõs is eighty* (Vol. 2, pp. 353–398). Budapest: János Bolyai Mathematical Society.

Mattia, D., Cincotti, F., Astolfi, L., De Vico Fallani, F., Scivoletto, G., Marciani, M.G., Babiloni, F. (2009). Motor cortical responsiveness to attempted movements in tetraplegia: evidence from neuroelectrical imaging. *Clinical Neurophysiology*, *119*, 2231–2237.

Middleton, F.A., & Strick, P.L. (2000). Basal ganglia and cerebellar loops: motor and cognitive circuits. *Brain Research. Brain Research Reviews*, *31*, 236–250.

Moretti, D.V., Babiloni, F., Carducci, F., Cincotti, F., Remondini, E., Rossigni, P.M., Salinari, S., Babiloni, C. (2003). Computerized processing of EEG-EOG-EMG artifacts for multi-centric studies in EEG oscillations and event-related potentials. *International Journal of Psychophysiology*, *47*, 199–216.

Muthukumaraswamy, S.D. (2010). Functional properties of human primary motor cortex gamma oscillations. *Journal of Neurophysiology*, *104*(5), 2873–2885.

Newman, M.E.J. (2003). The structure and function of complex networks. *SIAM Review*, *45*, 167–256.

Newman, M.E.J. (2005). A measure of betweenness centrality based on random walks. *Social Networks*, *27*, 39–54.

Noh, J.D., & Rieger, H. (2004). Random walks in complex networks. *Physical Review Letters*, *92*, 118701.

Nolte, G., Bai, U., Weathon, L., Mari, Z., Vorbach, S., Hallet, M. (2004). Identifying true brain interaction from EEG data using the imaginary part of coherency. *Clinical Neurophysiology*, *115*, 2294–2307.

Nunez, P.L., Srinivasan, R., Westdorp, A.F., Wijesinghe, R.S., Tucker, D.M., Silberstein, R.B., Cadusch, P.J. (1997). EEG coherency I: statistics, reference electrode, volume conduction, laplacians, cortical imaging, and interpretation at multiple scales. *Electroencephalography and Clinical Neurophysiology*, *103*, 499–515.

Ohara, S., Mima, T., Baba, K., Ikeda, A., Kunieda, T., Matsumoto, R., Yamamoto, J., Matsuhashi, M., Nagamine, T., Hirasawa, K., Hori, T., Mihara, T., Hashimoto, N., Salenius, S., Shibasaki, H. (2001). Increased synchronization of cortical oscillatory activities between human supplementary motor and primary sensorimotor areas during voluntary movements. *Journal of Neuroscience*, *21*(23), 9377–9386.

Pantazis, D., Nichols, T.E., Baillet, S., Leahy, R.M. (2005). A comparison of random field theory and permutation methods for the statistical analysis of MEG data. *Neuroimage*, *25*, 383–394.

Pfurtscheller, G., & Lopes da Silva, F.H. (1999). Event-related EEG/MEG synchronization and desynchronization: basic principles. *Clinical Neurophysiology*, *11*, 1842–1857.

Pollok, B., Gross, J., Schnitzler, A. (2002). Human cortical EEG rhythms during the observation of simple aimless movements. A high resolution EEG study. *Neuroimage*, *17*, 559–572.

Pollok, B., Gross, J., Schnitzler, A. (2006). How the brain controls repetitive finger movements. *Journal of Physiology - Paris*, *99*, 8–13.

Reijneveld, J.C., Ponten, S.C., Berendse, H.W., Stam, C.J. (2007). The application of graph theoretical analysis to complex networks in the brain. *Clinical Neurophysiology*, *118*, 2317–2331.

Rodrigues, F.A., & da Fontoura Costa, L. (2010). Generalized connectivity between any two nodes in a complex network. *Physical Review E*, *81*, 036113.

Schlögel, A., & Supp, G. (2006). Analyzing event-related EEG data with multivariate autoregressive parameters. In C. Neuper, & W. Klimesh (Eds.), *Progress in brain research* (Vol. 159, pp. 135–147). The Netherlands: Elsevier.

Schoffelen, J.M., & Gross, J. (2009). Source connectivity analysis with MEG and EEG. *Human Brain Mapping*, *30*, 1857–1865.

Sporns, O., Chialvo, D.R., Kaiser, M., Hilgetag, C.C. (2004). Organization, development and function of complex brain networks. *Trends in Cognitive Sciences*, *8*, 418–425.

Srinivasan, R., Nunez, P.L., Silberstein, R.B. (1998). Spatial filtering and neocortical dynamics: estimates of EEG coherence. *IEEE Transactions on Biomedical Engineering*, *45*, 814–826.

Stephenson, K., & Zelen, M. (1989). Rethinking centrality: methods and examples. *Social Networks*, *11*, 1–37.

Toppi, J., De Vico Fallani, F., Vecchiato, G., Maglione, A.G., Cincotti, F., Mattia, D., Salinari, S., Babiloni, F., Astolfi, L. (1989). Rethinking centrality: methods and examples. *Social Networks*, *11*, 1–37.

Valencia, M., Pastor, M.A., Fernández-Seara, M.A., Artieda, J., Martinerie, J., Chavez, M. (2009). Complex modular structure of large-scale brain networks. *Chaos*, *19*, 02311.

van Wijk, B.C.M., Stam, C.J., Daffertshofer, A. (2010). Comparing brain networks of different size and connectivity density using graph theory. *PLoS ONE*, *5*, e13701.

Varela, F., Lachaux, J.-P., Rodriguez, E., Martinerie, J. (2001). The brainweb: phase synchronization and large-scale integration. *Nature Reviews Neuroscience*, *2*, 229–239.

Wolpert, D.M., Ghahramani, Z., Jordan, M.I. (1995). An internal model for sensorimotor integration. *Science*, *269*, 1880–1882.

Zamora-López, G., Zhou, C., Kurths, J. (2009). Graph analysis of cortical networks reveals complex anatomical communication substrate. *Chaos*, *19*, 015117.